On the calibration of DC resistance ratio bridges

Measurement 223 (2023) 113664

Contents lists available at ScienceDirect

Measurement

journal homepage: www.elsevier.com/locate/measurement

On the calibration of DC resistance ratio bridges

M. Marzano *, C. Cassiago, V. D'Elia, E. Gasparotto, L. Callegaro

Istituto Nazionale di Ricerca Metrologica (INRIM), Strada delle Cacce, 91 10135 Torino, Italy

ARTICLE INFO

Keywords:
Resistance measurement
Electrical instruments
Measurement units and standards
84.37.+q
07.50.-e
06.20.F

ABSTRACT

Current comparator bridges are employed for the realization of the resistance scale from the quantum Hall effect in several National Metrology Institutes and calibration centers. Quantum resistance standards under development, based on novel materials and tabletop dry cryostats, make the more achievable DC current comparator bridges (DCCs) a viable alternative to the more accurate but more expensive cryogenic current comparator bridges (CCCs). A DCC ratios' calibration against a reference CCC is a straightforward way to improve the DCC's performances and the resistance scale overall accuracy.

The paper reports the calibration results of two DCCs on the ratios employed in a 1 Ω to 10 kΩ resistance scale traceable to a 12.906 kΩ quantized Hall resistance, showing a good reproducibility and stability of the DCC readings over the measurement period and supporting the possibility of a DCC errors' correction and of a realization of the primary resistance scale at the 10^{-8} level.

1. Introduction

The basis of primary dc resistance metrology is the realization of the SI unit of resistance with the quantum Hall effect, and the calibration of a resistance scale maintained by artifact resistance standards. Both tasks are performed with dc resistance ratio bridges. In the midrange resistance scale (from 1 Ω to 10 kΩ) modern metrology laboratories typically rely on dc current comparator resistance bridges.

In a current comparator [1] the currents I_1 and I_2 flow through windings having N_1 and N_2 turns, and generate two magnetomotive forces $N_1 I_1$ and $N_2 I_2$ in opposite directions. A null flux condition is achieved when $N_1 I_1 = N_2 I_2$.

In a current comparator resistance bridge such null flux condition is maintained by a control loop. The currents flow through the two resistors R_1 and R_2 to be compared, and the turns ratio N_1/N_2 is selected to be close to the ratio R_1/R_2, so that voltages $V_1 = R_1 I_1$ and $V_2 = R_2 I_2$ have similar magnitude. The small voltage residual $\Delta V = V_1 - V_2$ gives the bridge reading; the bridge can either operate by a direct reading of ΔV, or by reducing its magnitude with an additional control loop.

Two major classes of current comparator bridges are available:

DCC bridges, DC current comparator resistance bridges. In these instruments the magnetic flux generated by the windings follows a path determined by a high-permeability ferromagnetic core and shields. The magnetic balance condition is sensed with a fluxgate technique [2].

DCC bridges can be operated at room temperature. Fully-automated commercial versions are available; typically, available bridge ratios do not extend much beyond the 0.1 to 10 range. The specified accuracy is of parts in 10^7 to 10^8.

CCC bridges, Cryogenic current comparator resistance bridges [3]. The flux path is determined by the Meissner effect in superconducting shields; the magnetic balance is sensed by a superconducting quantum-interference device (SQUID) magnetometer.

CCC bridges are typically semi-automated; commercial versions are available. Available ratios can cover the 10^{-3} to 10^3 range. They are more expensive than DCCs and the operating costs are boosted by the need of liquid helium supply to achieve the cryogenic temperatures, and well-trained operators. The base accuracy is of a few parts in 10^9.

The established implementation for the realization of the resistance unit with the quantized Hall resistance (QHR) is with GaAs/AlGaAs heterostructure devices in low temperatures (1.5 K or lower) with a strong magnetic field (around 10 T, typically). It is therefore typically limited to national metrology institutes, where the cryogenic laboratory facilities and professional skills required are shared by both the QHR

* Corresponding author.
E-mail address: m.marzano@inrim.it (M. Marzano).

[1] Regarding the liquid helium consumption a charge of 100 L of helium allows for 2–3 weeks of operation of a CCC, but only 3–5 days of operation of a 10 T QHE cryomagnet.

https://doi.org/10.1016/j.measurement.2023.113664
Received 25 July 2023; Received in revised form 18 September 2023; Accepted 2 October 2023
Available online 17 October 2023

and the CCC operation. The resources absorbed by the CCC operation are therefore a minor fraction of those of the whole implementation.[1]

In the last few years, however, QHE metrology research focused on graphene devices, which can operate at higher temperatures and lower magnetic fields [4]; high-accuracy QHE experiments in tabletop dry cryostats have been performed [5]. Very recently, measurements of the quantum anomalous Hall effect [6] in topological insulators show that an accurate quantum resistance standard can be achieved [7] with a small permanent magnet. Such developments forecast future low-cost, easy-to-operate quantum resistance standards in compact dry cryostats, affordable also by smaller national metrology institutes, calibration centers and industry. In this new framework, the operating costs of a CCC might become a major bottleneck for a widespread realization of a resistance unit and scale. DCCs represent thus the most viable alternative.

DCCs are less performant in terms of accuracy than CCCs. A calibration of the DCC bridge ratio readings using the more accurate CCC as a reference ratio standard can be the most straightforward way to improve the DCC performances.

This paper reports a calibration exercise of two models of a commercial DCC bridge, performed by comparison with a reference CCC bridge. The calibration method proceeds by measuring the value of the resistance ratio between two thermostated resistors with the DCC and with the CCC, with the same measurement currents and in short temporal sequence. The method has been considered in literature [5,8] and is here analyzed in detail.

The calibration determines the DCC bridge ratio error with an uncertainty in the order of 1×10^{-8}. The known error values, if sufficiently stable versus time, can be employed to correct the DCC readings when employed for the realization of the resistance scale or for calibration for customers, thus improving the measurement reliability and uncertainty with respect to the case when the sole DCC bridge specifications are employed.

The results here reported focus on the specific ratio 12.906 kΩ:1 kΩ and on 10:1 ratios over the range 1 Ω to 10 kΩ. Since 12.906 kΩ is approximately the value of the quantized Hall resistance in GaAs or graphene devices, the ratios allow the realization of a maintained decadal resistance scale from 1 Ω to 10 kΩ.

2. Instruments and standards

2.1. CCC bridge

The CCC bridge employed is manufactured by Magnicon GmbH on design of the Physikalisch-Technische Bundesanstalt (PTB). The windings turn numbers are selected by manually composing them, by connecting in series (or anti-series) individual winding sections having turn numbers in an (approximate) binary sequence; up to about 4646 turns can be achieved. Fractional turn numbers are simulated by a compensation network. After this initial manual setup, the measurement process is automated. The base ratio accuracy is in the 10^{-9} range.

2.2. DCC bridge

Two DCC bridges, a Measurement International MI6010B purchased in 2006 and MI6010D purchased in 2021, have been employed in the calibration exercise. These models are widespread in calibration laboratories.[2] The specified measurement range of the MI6010B is 1 mΩ to 13 kΩ; that of MI6010D is 1 mΩ to 100 kΩ.

[2] A higher-accuracy model, MI6020Q, is available from the same manufacturer

2.3. Resistance standards

The standard resistors employed are:

- STR1, a tailored resistor with a nominal value of 12.906 kΩ, constructed from an Electro Scientific Industries (now IET Labs) model ESI SP5120. The resistor is enclosed in a thermostatic air bath with a nominal temperature of 27 °C with a stability within a few mK.
- STD VH01, a custom-made resistor with a nominal value of 1 kΩ, made from the parallel of 10 Vishay VHA 512T 10 kΩ components (tolerance ±0.005%) thermostated at about 27 °C.
- Tinsley mod. 5685 Wilkins-type [9] standard resistors of 1 Ω, 10 Ω, 100 Ω, 1 kΩ, 10 kΩ nominal value. They are electrically shielded and kept in a temperature-stabilized chamber at the nominal temperature of 23 °C with 5 mK short-term stability.

3. Experimental

The calibration is performed by measuring in short temporal sequence the resistance ratio with the DCCs and with the CCC, which acts as reference ratio standard. The calibration value δ_c is the deviation

$$\delta_c = \frac{Q_{DCC} - Q_{CCC}}{Q_{nom}} \quad (1)$$

of Q_{DCC}, the ratio reading from the DCC bridge, from Q_{CCC}, the corresponding reading from the CCC bridge, relative to the nominal ratio Q_{nom}.

4. Uncertainty

The contributions to the calibration uncertainty are the uncertainty reference ratio measurement provided by the CCC, the statistical uncertainty of the readings of the DCC in the course of the calibration event, and the uncertainty associated to the stability and definability of the resistors employed as transfer standards.

4.1. CCC uncertainty

The expression of uncertainty of a CCC measurement is considered in several papers [10–14]. A full discussion is beyond the scope of this paper, we briefly summarize here the main uncertainty contributions:

Main current ratio. The comparator current ratio in the main windings when at equilibrium is identified with the (inverse) turns ratio; a small uncertainty, related to possible flux leakages [3], is assigned.

Compensation turn ratio. A similar effect can occur in the compensation winding, employed to increase the current ratio resolution, see below.

Compensation network. The CCC includes an active network to achieve an equivalent fractional turns ratio. The gain error of the network [11,12] is a source of uncertainty.

ΔV detector. The CCC reading is the voltage deviation from equilibrium ΔV, given by a nanovoltmeter, which gain accuracy is considered.

Flux detector. The SQUID is an intrinsically nonlinear device. The automated control loops of the SQUID electronics linearize its response. The residual nonlinearity can rectify a fraction of the flux noise, which can give an offset to the perfect zero flux condition [13]. This effect is conservatively quantified in a maximum deviation of 20 $\mu\Phi_0$, which enters the uncertainty budget as an apparent deviation of ΔV. The sensitivity coefficient is dependent on the flux linkage sensitivity of the SQUID (about 11 $\mu A/\Phi_0$), and the CCC measuring currents and turn numbers [15].

Current source. ΔV is normalized to one of the current source settings, which have a finite setting accuracy.

4.2. DCC type a uncertainty

The time series of the DCC readings show a significant degree of autocorrelation, so the standard deviation of the mean is not a reliable estimator of the Type A uncertainty of the DCC. The approach proposed in [16] has been followed. More details are given in [17].

4.3. Resistance standards

The short-term stability of the resistors during the comparison is a source of measurement uncertainty. For simplicity, to each calibration point a fixed duration of $\Delta t = 6\,\mathrm{h}$ is assigned.

The following influence quantities and effects are considered:

Temperature. The effect is evaluated by considering a maximum temperature deviation in the thermostating bath $\pm\Delta T$ with respect to a reference temperature T_{ref}, and evaluating for each of the resistors the maximum relative resistance deviation

$$\Delta R_{\mathrm{T}} = \max\left|\alpha\left(T \pm T_{\mathrm{ref}}\right) + \beta\left(T \pm T_{\mathrm{ref}}\right)^2\right|, \quad (2)$$

where α and β are the linear and quadratic temperature coefficients of each resistor.

The uncertainty contribution related to the temperature stability of each resistor is the standard deviation of a uniform distribution with semiamplitude ΔR_{T}.

Pressure. The effect is evaluated by considering a maximum pressure deviation $\Delta p = 4\,\mathrm{hPa}$ in the course of the duration Δt of the comparison. The pressure coefficients c_{p} of the specific resistors employed are unknown. A maximum c_{p} of $\pm 1\times 10^{-9}\,\mathrm{hPa}^{-1}$ has been guessed on the basis of literature values.[3]

The uncertainty contribution related to the pressure stability of each resistor is the standard deviation of a uniform distribution with semiamplitude $\Delta R_{\mathrm{p}} = c_{\mathrm{p}}\Delta p$.

Isolation. The isolation of the connecting cables, of the resistors, and of the measuring instruments themselves with respect to the environment can cause current leakages. A full evaluation of the effect of the various isolation resistances is beyond the scope of this paper. The uncertainty contribution is evaluated as the effect of an unknown isolation resistance, minimum value $10\,\mathrm{T\Omega}$, on the higher-value resistor involved in the measurement.

Power. The power dissipated in a resistor influence its value by raising the local temperature with respect to the environment. The time constant of the phenomenon can be comparable with the measurement time. Although DCC and CCC measurements are performed at the same power levels, the exchange of the two instruments require some time, and thus power is cycled, and thus the measurement might be performed with the resistors in a slightly different temperature rise condition. With the currents selected for the measurements, the effect is of significance only for resistors at or below $1\,\mathrm{k\Omega}$ nominal value. The uncertainty contribution to the measurement is evaluated as the effect of a power coefficient of unknown sign and maximum magnitude $|c_{\mathrm{P}}| = 1\times 10^{-6}\,\mathrm{W}^{-1}$ on the resistor having lower value (the one dissipating the larger power).

[3] The pressure coefficients of several $100\,\Omega$ Tinsley 5685 A resistors are reported in [18], the largest one being of $-1.8\times 10^{-10}\,\mathrm{hPa}^{-1}$. The pressure effects on a $10\,\mathrm{k\Omega}$ Tinsley 5685B resistor are provided by [19]; a nonlinear dependence is observed, a maximum coefficient of $5\times 10^{-10}\,\mathrm{hPa}^{-1}$ around ambient pressure can be inferred. The pressure coefficient of three ESI/TEGAM $10\,\mathrm{k\Omega}$ resistors, the largest being of $-6\times 10^{-10}\,\mathrm{hPa}^{-1}$, are given in [20].

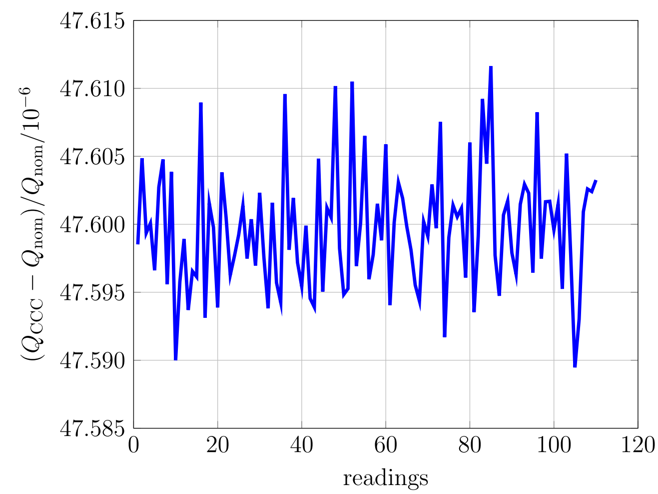

Fig. 1. Time series of the readings given by the CCC, when performing a $12.906\,\mathrm{k\Omega}$:$1\,\mathrm{k\Omega}$ measurement at $50\,\mu\mathrm{A}$ (on the highest resistor under test).

Time drift. This is evaluated as the maximum drift in the course of the duration Δt of the comparison, as a fraction of the yearly relative drift c_{t}. For the resistors in the $1\,\Omega$ to $10\,\mathrm{k\Omega}$ range the manufacturer specifications ($c_{\mathrm{t}} = 2\times 10^{-6}\,\mathrm{yr}^{-1} = 2.3\times 10^{-10}\,\mathrm{h}^{-1}$) is considered. For the STR1 standard, long-term behavior (> 10 yr of observation) shows that the drift over Δt is negligible. The uncertainty contribution related to the time stability of each resistor is the standard deviation of a uniform distribution with semiamplitude $\Delta R_{\mathrm{t}} = c_{\mathrm{t}}\Delta t$.

For simplicity, no correlation between the effects on the two resistors employed in the comparison have been considered.

The linear and quadratic temperature coefficients and the yearly relative drift of the employed resistors are provided as a Supplementary File.

5. Results

5.1. Individual measurements

Figs. 1 and 2 gives an example of the time series of measurements performed with the three instruments involved in the comparison, for the $12.906\,\mathrm{k\Omega} : 1\,\mathrm{k\Omega}$ comparison. As anticipated in Section 4.2, DCC time series show a significant internal correlation, which has been taken into account in the expression of the type A measurement uncertainty.

5.2. Calibration results

Fig. 3 gives the outcome of the calibration exercise for the two bridges, that is the deviation δ_{c} of the DCC measurement from the CCC ones, together with the combined uncertainty, measured for different ratios and over different periods of time. In the $12.906\,\mathrm{k\Omega} : 1\,\mathrm{k\Omega}$ comparison, the STR1 and STD VH01 resistors were involved. In the other comparisons, the Tinsley mod. 5685 Wilkins-type [9] standard resistors of $1\,\Omega$, $10\,\Omega$, $100\,\Omega$, $1\,\mathrm{k\Omega}$, $10\,\mathrm{k\Omega}$ nominal value were involved. The same data in numerical form are provided as a Supplementary File.

Table 1 gives two examples of uncertainty budgets, expressed as stated in Section 4 for the calibrated ratio error δ_{c}. The uncertainty for all ratios is smaller than 2×10^{-8}; for high resistance values the most relevant uncertainty contribution is that of the DCC readings, whereas for low resistance values the main contribution is related to the power coefficient of the lower-value resistor being measured.

The calibration results show a high short-term (days) reproducibility; the deviations over the observation period of seven months is

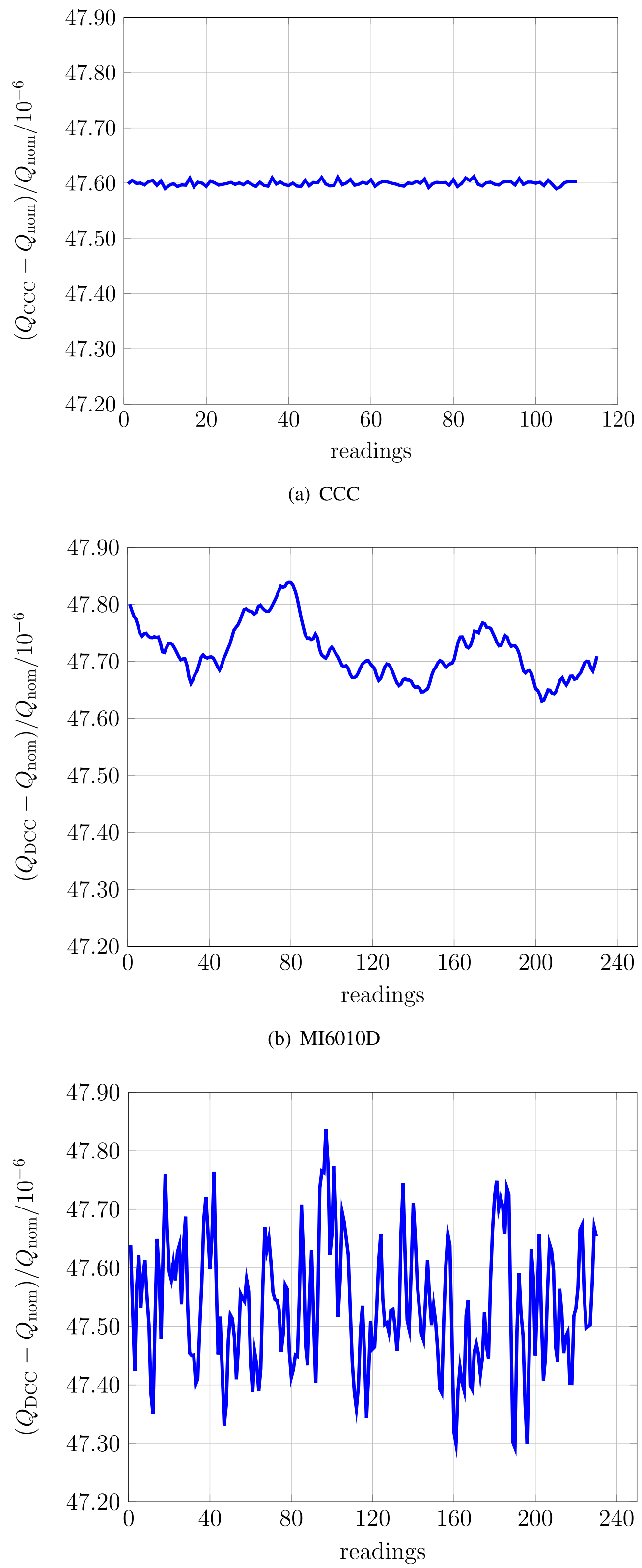

(a) CCC

(b) MI6010D

(c) MI6010B

Fig. 2. Time series of the readings given by the three instruments involved in the calibration exercise, when performing a 12.906 kΩ:1 kΩ measurement at 50 μA. Fig. 2(a) gives the same data of Fig. 1, the vertical scale being adjusted to be the same of Figs. 2(b) and 2(c) for ease of comparison.

Table 1
Uncertainty budget of the calibration value δ_c for the bridge MI6010D bridges when measuring the ratios 12.906 kΩ:1 kΩ and 100 Ω:10 Ω, on dates of 12 and 7 Jun 2023 respectively. See Section 4 for the description of the uncertainty components. Standard uncertainty is considered (coverage factor $k = 1$).

Contribution	12.906:1 kΩ $u_k(\delta_c)/10^{-9}$	100:10 Ω $u_k(\delta_c)/10^{-9}$	Type
CCC bridge			
Reading	0.4	0.1	A
Main current ratio	<0.1	<0.1	B
Comp. turn ratio	<0.1	<0.1	B
Comp. network	<0.1	<0.1	B
ΔV detector	<0.1	<0.1	B
Flux detector	1.2	0.2	B
Current source	<0.1	<0.1	B
DCC bridge			
Reading time series	14.0	1.7	A
Resistance standards			
Temperature	0.5	0.4	B
Pressure	1.6	1.6	B
Isolation	0.6	<0.1	B
Power	0.2	5.2	B
Time drift	1.1	1.1	B
$u(\delta_c)$	15.0	6.0	comb.

limited (below two times the standard uncertainty); future observation will tell whether these deviations are related to a drift over time or are random effects.

6. Discussion and conclusions

The calibration exercise shows that it is possible to calibrate the ratio error of commercial DCC bridges by comparison with a CCC. The measured errors have a good reproducibility over a measurement period (a few days) and show a reasonable stability between two measurement periods separated by about 7 months of time. Such stability is a good basis to perform in-use corrections to the DCC readings on the basis of the calibrated values. A longer-term observation of the DCC items will confirm this possibility. If the DCC is employed to generate a resistance scale, the DCC calibration can improve the uncertainty of the calibrated resistance values. The proper assignment of an in-use uncertainty of resistance measurements performed with a calibrated DCC goes beyond the scope of this paper.

The calibration exercise covers the ratios required to realize a primary resistance scale between 1 Ω and 10 kΩ with traceability to the quantum Hall effect, with an uncertainty of one or few parts in 10^8. Such uncertainty level is in line with the Calibration and Measurement Capabilities claims of National Metrology Institutes as declared in the Key Comparison DataBase (KCDB) [21] and the Degrees of Equivalence of the international comparison BIPM.EM-K13 [22].

DCC bridges, together with AC transformer ratio bridges [23] [24, Sec. 4], are widely employed in primary temperature metrology. They are employed to measure the ratio between the resistance of standard platinum resistance thermometers (SPRTs) and a reference resistor, and play a critical role in the realization of the ITS-90 temperature scale. The calibration method proposed can be applied to thermometry bridges as complementary to the more common Resistance Bridge Calibrator [25,26] method. The ratios of interest are not limited to decadic values, hence non-decadic resistance standards would be required. If ac transformer ratio bridges are to be calibrated, the ac–dc dependence of the resistors, and the different power dissipation must also be considered.

CRediT authorship contribution statement

M. Marzano: Conceptualization, Formal analysis, Methodology, Visualization, Writing – original draft, Writing – review & editing. **C. Cassiago:** Methodology, Validation. **V. D'Elia:** Investigation, Methodology.

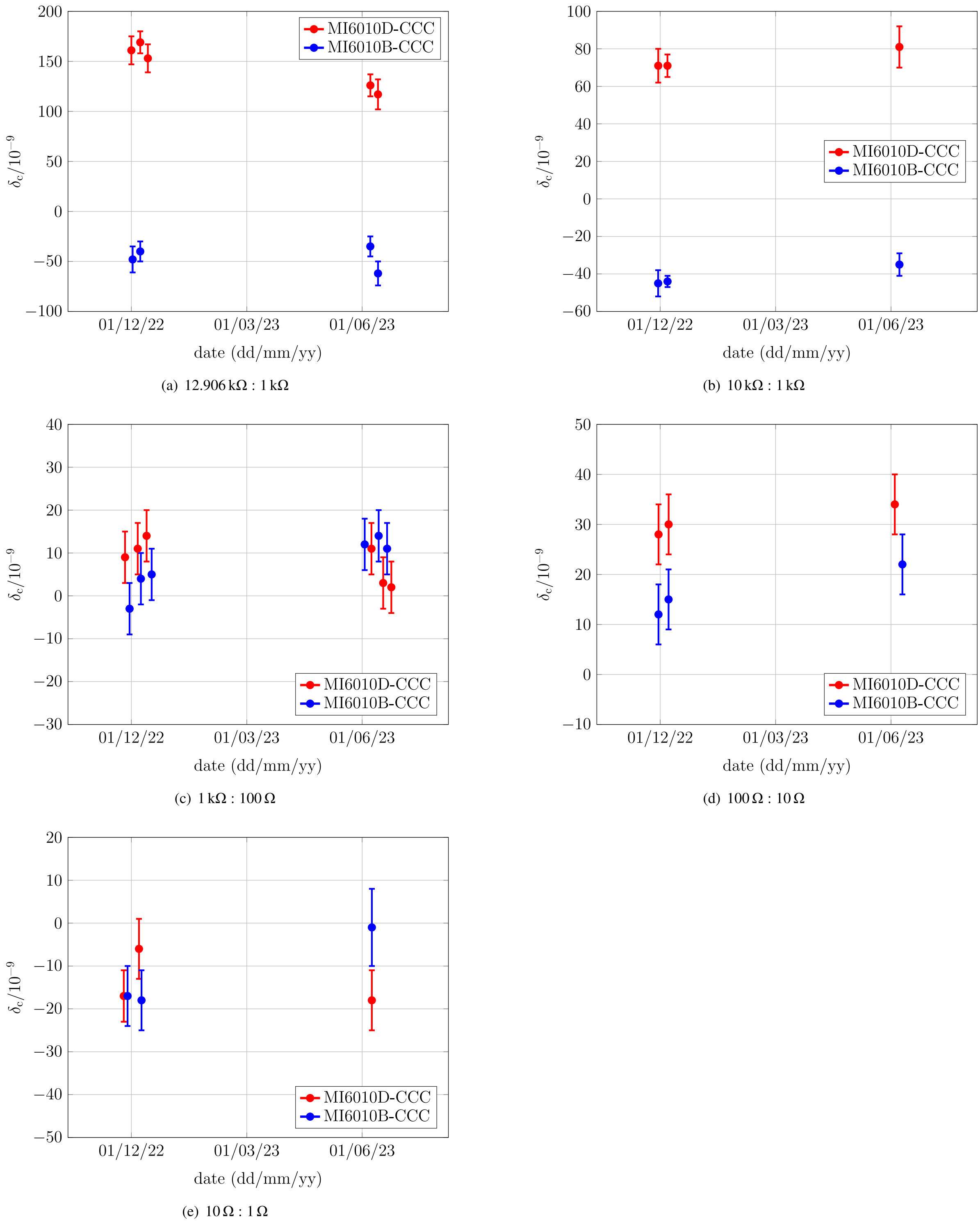

Fig. 3. Outcome of the calibration. δ_c is the relative difference between the DCC and the CCC measurement, versus the measurement date. The measurements presented in (a)–(e) are performed at 50 µA, 100 µA, 1 mA, 3 mA and 10 mA (on the highest resistor under test), respectively. The uncertainty bars display the standard uncertainty ($k = 1$).

E. Gasparotto: Investigation, Methodology. **L. Callegaro:** Supervision, Funding acquisition, Software.

Declaration of competing interest

The authors declare that they have no known competing financial interests or personal relationships that could have appeared to influence the work reported in this paper.

Data availability

The research data are reported in the Supplementary Data File in appendix.

Acknowledgments

This work has been supported by the project CAPSTAN Quantum electrical Italian national capacitance standard funded by the MIUR

Progetti di Ricerca di Rilevante Interesse Nazionale (PRIN) Bando 2020, Italy, grant 2020A2M33J.

The authors are indebted to Martn Götz, Physikalisch-Technische Bundesanstalt (PTB), Germany, for help in the expression of the CCC uncertainty.

Appendix A. Supplementary data

Supplementary material related to this article can be found online at https://doi.org/10.1016/j.measurement.2023.113664.

References

[1] W.J.M. Moore, P.N. Miljanic, The Current Comparator, in: IEE Electrical Measurement Series, vol. 4, Peter Peregrinus Ltd, London, UK, 1988, ISBN 0863411126.
[2] M.P. MacMartin, N.L. Kusters, A direct-current-comparator ratio bridge for four-terminal resistance measurements, IEEE Trans. Instr. Meas. 15 (4) (1966) 212–220.
[3] J.M. Williams, Cryogenic current comparators and their application to electrical metrology, IET Sci. Meas. Technol. 5 (2011) 211–224.
[4] R. Ribeiro-Palau, F. Lafont, J. Brun-Picard, D. Kazazis, A. Michon, F. Cheynis, O. Couturaud, C. Consejo, B. Jouault, W. Poirier, F. Schopfer, Quantum Hall resistance standard in graphene devices under relaxed experimental conditions, Nat. Nanotech. 10 (2015) 965—971.
[5] A.F. Rigosi, A.R. Panna, S.U. Payagala, M. Kruskopf, M.E. Kraft, G.R. Jones, B.-Y. Wu, H.-Y. Lee, Y. Yang, J. Hu, D.G. Jarrett, D.B. Newell, R.E. Elmquist, Graphene devices for tabletop and high-current quantized Hall resistance standards, IEEE Trans. Instr. Meas. 68 (6) (2019) 1870–1878.
[6] H. Chi, J.S. Moodera, Progress and prospects in the quantum anomalous Hall effect, APL Mater. 10 (9) (2022) 090903.
[7] Y. Okazaki, T. Oe, M. Kawamura, R. Yoshimi, S. Nakamura, S. Takada, M. Mogi, K.S. Takahashi, A. Tsukazaki, M. Kawasaki, Y. Tokura, N.-H. Kaneko, Quantum anomalous Hall effect with a permanent magnet defines a quantum resistance standard, Nat. Phys. 18 (1) (2022) 25–29.
[8] A.R. Panna, M.E. Kraft, A.F. Rigosi, G.R. Jones, S.U. Payagala, M. Kruskopf, D.G. Jarrett, R.E. Elmquist, Uncertainty of the ohm using cryogenic and non-cryogenic bridges, in: 2018 Conference on Precision Electromagnetic Measurements, CPEM 2018, 2018, pp. 1–2.
[9] F.J. Wilkins, M.J. Swan, Resistors having a calculable performance with frequency, Proc. IEE 116 (1969) 318–324.
[10] J.M. Williams, T.J.B.M. Janssen, G. Rietveld, E. Houtzager, An automated cryogenic current comparator resistance ratio bridge for routine resistance measurements, Metrologia 47 (3) (2010) 167.
[11] D. Drung, M. Götz, E. Pesel, H.J. Barthelmess, C. Hinnrichs, Aspects of application and calibration of a binary compensation unit for cryogenic current comparator setups, IEEE Trans. Instr. Meas. 62 (10) (2013) 2820–2827, http://dx.doi.org/10.1109/TIM.2013.2259112.
[12] M. Götz, D. Drung, Stability and performance of the binary compensation unit for cryogenic current comparator bridges, IEEE Trans. Instr. Meas. 66 (6) (2017) 1467–1474.
[13] C. Sanchez, Reassessment of the uncertainties of the NRC cryogenic current comparator and quantum Hall resistance standard, in: 2018 Conference on Precision Electromagnetic Measurements, CPEM 2018, 2018, pp. 1–2.
[14] W. Poirier, D. Leprat, F. Schopfer, A resistance bridge based on a cryogenic current comparator achieving sub-10^{-9} measurement uncertainties, IEEE Trans. Instr. Meas. 70 (2021) 1–14, http://dx.doi.org/10.1109/TIM.2020.3010111.
[15] D. Drung, M. Götz, E. Pesel, H. Scherer, Improving the traceable measurement and generation of small direct currents, IEEE Trans. Instrum. Meas. 64 (11) (2015) 3021–3030, http://dx.doi.org/10.1109/tim.2015.2440564.
[16] N.F. Zhang, Calculation of the uncertainty of the mean of autocorrelated measurements, Metrologia 43 (4) (2006) S276–S281.
[17] M. Marzano, P.P. Capra, C. Cassiago, V. D'Elia, E. Gasparotto, L. Callegaro, Metrological assessment of DC current comparator resistance bridges, Measurement 215 (2023) 112858.
[18] B. Schumacher, Final report on EUROMET.EM-K10: Key comparison of resistance standards at $100\,\Omega$, Metrologia 47 (1A) (2010) 01008.
[19] P.P. Capra, R. Cerri, F. Galliana, M. Lanzillotti, A. Pollarolo, P. Roccato, Measurement setup to characterize electrical standards, in: 19th International Congress of Metrology (CIM2019) Proceedings, Paris, France, 2019, p. 11003.
[20] R.F. Dziuba, Pressure dependencies of standard resistors, in: Proc. of the National Conference of Standards Laboratories Workshop and Symposium (NCSL) Conference, Albuquerque, NM, USA, 1993.
[21] The BIPM Key Comparison DataBase (KCDB) in support of the CIPM Mutual Recognition Arrangement. kcdb.bipm.org.
[22] The BIPM Key Comparisons of electrical resistance standards using $1\,\Omega$ and $10\,k\Omega$ resistors as travelling standards (BIPM.EM-K13.a and b). www.bipm.org/kcdb/comparison?id=1780.
[23] J.J. Hill, A.P. Miller, An a.c. double bridge with inductively coupled ratio arms for precision platinum-resistance thermometry, Proc. Inst. Electr. Eng. 110 (2) (1963) 453, http://dx.doi.org/10.1049/piee.1963.0068.
[24] L. Callegaro, Electrical Impedance: Principles, Measurement, and Applications, in: Series in Sensors, CRC Press, 2013.
[25] D.R. White, K. Jones, J.M. Williams, I.E. Ramsey, A simple resistance network for calibrating resistance bridges, IEEE Trans. Instrum. Meas. 46 (5) (1997) 1068–1074, http://dx.doi.org/10.1109/19.676712.
[26] J.V. Pearce, J. Gray, R.I. Veltcheva, Characterisation of a selection of AC and DC resistance bridges for standard platinum resistance thermometry, Int. J. Thermophys. 37 (11) (2016) http://dx.doi.org/10.1007/s10765-016-2113-6.